

# Hydrogen induced effect on ZnTe/Co bilayer thin films

S. P. NEHRA<sup>a,b,\*</sup>, M. S. DHAKA<sup>c</sup>, ANSHU SHARMA<sup>a</sup>, NEERAJ KUMAR<sup>d</sup>, RITU MALIK<sup>b</sup>, M. SINGH<sup>a</sup>

<sup>a</sup>Department of Physics, University of Rajasthan, Jaipur -302055, India

<sup>b</sup>Centre of Excellence for Energy and Environmental Studies,

Deenbandhu Chhotu Ram University of Science and Technology, Murthal, Sonapat-131039, India

<sup>c</sup>Department of Physics, University College of Science,

Mohanlal Sukhadia University, Udaipur-313001, India

<sup>d</sup>Tata Institute of Fundamental Research, Mumbai-400005, India

Hydrogen is an amphoteric impurity and acts as a source of doping. It affects the electrical, optical and magnetic properties of materials. This paper reports the effect of hydrogen in electrical, optical and magnetic properties of ZnTe/Co bilayer thin films. These thin films were deposited on glass substrates using thermal evaporation technique. Hydrogenation has been incorporated at different pressure of hydrogen for half an hour under constant temperature of 333 K. Electrical, optical and magnetic properties of these films have been studied. The conductivity values have been found to be decreased from  $3.04 \times 10^{-4} \Omega^{-1} \text{cm}^{-1}$  to  $2.42 \times 10^{-4} \Omega^{-1} \text{cm}^{-1}$  and optical band gap values have been found to be increased from 3.33 eV to 3.38 eV due to hydrogen passivation effect. Presence of magnetic element has been confirmed by superconducting quantum interference device and X-ray diffraction measurements. Hydrogenation effect on these BLs thin films has also been confirmed using Raman Spectroscopy. Surface topography has been observed by optical microscopy.

(Received August 23, 2013; accepted January 22, 2014)

**Keywords:** Bilayer thin films, Hydrogenation, I-V characteristics, Optical properties, Magnetization and surface topography

## 1. Introduction

In today's information world, data are processed by semiconductor chips. But tomorrow's information technology data will be processed by 'spintronic' device that exploits both charge and 'spin' to carry data [1]. Semiconductor spin electronics is one of the most perspective directions for the modern technique development [2]. Diluted magnetic semiconductors (DMSs) are semiconductors with some magnetic ions as impurities in the host lattice [3]. The advantages of diluted magnetic semiconductor (DMS) based spin-electronic devices include enabling of instant-on computer, increased integration density, higher data processing speed, low electrical energy demand and compatibility of their fabrication processes with those currently used in industry [4]. The first known such DMS are II-VI and III-V semiconductors diluted with magnetic ions like Mn, Fe, Co, Ni, etc. Most of these DMS exhibit very high electron and hole mobility and thus useful for high speed electronic devices [5]. The magneto-optical effect in dilute magnetic semiconductors (DMSs) is directly related to the interaction between the d electrons of the transition metal ions and the s, p electrons of the host semiconductor [6]. There has been intense interest in the development of multilayer thin films over the past few decades, both because of the fundamental properties that such films display and because of their potential use in a range of diverse technological applications [7]. Pakhomov et al [8] reported a study of magnetic and transport properties of multilayer made by alternating deposition of ZnO and Co layers. They found that increasing the relative nominal thickness of Co layers leads to a cross-over from a DMS

superlattice, with the Curie temperature higher than 300 K. Several researchers studied the preparation and characterization of Mn doped ZnTe diluted magnetic semiconductors [9, 10].

Hydrogen passivation is a good method for investigating the origin of ferromagnetism in dilute magnetic semiconductors. Recently, the effect of hydrogen on the magnetic properties of several DMS was extensively investigated [11-13]. It was motivated by the fact that in the fabrication of thin films or electronic devices, samples actually are rarely free from hydrogen infectivity and hydrogen impurities are certainly introduced into thin films [14]. Molecular hydrogen was directly observed by Vetterhoffer et al [15] in crystalline GaAs by Raman spectroscopy. At  $T = 77 \text{ K}$ , GaAs samples those have been exposed to a hydrogen deuterium plasma exhibit four vibrational lines at 2842.6, 3446.5, 3925.9, and 3934.1  $\text{cm}^{-1}$ , respectively. Several researchers have been investigated hydrogenation effect on magnetic properties of diluted magnetic semiconductors [16-23].

In our previous articles [24-28] the effect of hydrogen on structural, electrical, optical and magnetic properties of BLs/MLs thin films have been studied. Raman spectra and surface morphology due to the hydrogenation of BLs/MLs thin films have also been reported. In this article, the effect of hydrogen on the electrical, optical and magnetic properties of ZnTe/Co BLs thin films has presented. Effect of hydrogenation on these thin films has also been studied with the help of Raman spectra and optical micrographs.

## 2. Experimental details

### 2.1 Sample preparation

Bilayer ZnTe/Co thin films with a thickness of 350 nm (200nm ZnTe/150 nm Co) were deposited onto glass substrates using vacuum coating unit. Hydrogenation process has been carried out in a labmade cell for 30 minutes at different pressure of hydrogen. Before the hydrogenation process takes place, a vacuum of the order of  $10^{-5}$  torr was maintained inside the cell then hydrogen gas introduced into cell. During hydrogenation, the films were kept at 333 K.

### 2.2 Characterization

The X-ray diffraction (XRD) patterns of as grown and hydrogenated thin films were recorded with the help of PANalytical X'pert PRO MPD PW3040/60 X-ray diffractometer using  $\text{CuK}_\alpha$  radiation. The XRD patterns of these films were taken in the range of angle ( $2\theta$ )  $20^\circ$  to  $80^\circ$ . Transverse I-V characteristics of as grown hydrogenated and annealed hydrogenated samples have been recorded using Keithley-238 high current source measuring unit. Electrical contacts were made by using conductive silver paste on the periphery of the samples. The absorption spectra of as deposited, annealed and hydrogenated thin films were carried out with the help of Hitachi Spectrophotometer U-3300. A superconducting quantum interference device (SQUID) system MPMS from Quantum Design, was employed to investigate the magnetic properties of these thin films.

Complementary results were obtained by Raman spectroscopy and optical microscopy. Raman spectra of as-grown and hydrogenated samples were taken by a Raman system (model -3000) having a Green laser beam of wavelength 532 nm. The optical micrographs have been observed with the help of Labomed optical microscope at 10x magnification having resolution of the order of  $1\mu\text{m}$  and the microscope was kept in reflection mode. Recorded two-dimensional (2-D) optical micrographs have been converted in three-dimensional (3-D) images with the help of Scanning Probe image Processor computer program.

## 3. Results and discussion

### 3.1 X-Ray Diffraction (XRD) measurements

The typical XRD patterns of as-grown and hydrogenated ZnTe/Co bilayer thin films are given in Fig. 1. As-grown thin film shows amorphous nature (Fig. 1a) while hydrogenated at 30 psi ZnTe/Co bilayer thin film show nanocrystalline structure due to annealing effect (Fig. 1b). The diffraction peaks at  $2\theta$  angles of  $25.24^\circ$  and  $27.55^\circ$  correspond to (002) and (101) planes of hexagonal wurzite structure of ZnTe have been observed. Plane (111) has also been observed corresponding to angle  $2\theta = 44.27^\circ$

for cubic cobalt. The crystallite size as calculated from Scherrer's formula for the highest intensity peak at  $2\theta = 27.55^\circ$  is 6.15nm. The micro strain for peak at  $2\theta = 27.55^\circ$  as calculated from Stokes and Wilson formula,

$$\epsilon_{str} = \frac{\beta}{4\tan\theta}$$

is found 0.2430.

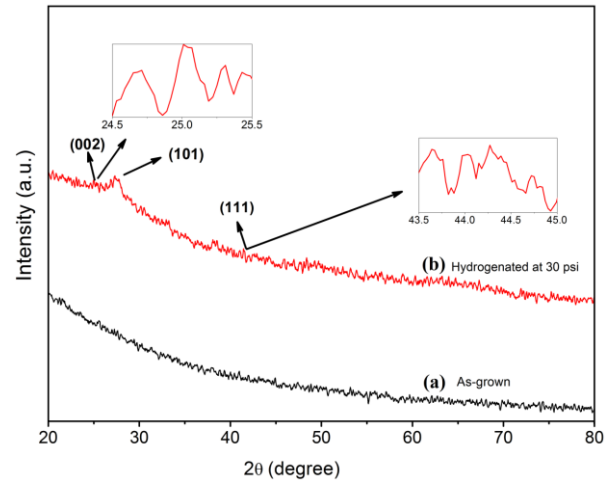


Fig. 1. X-ray diffraction pattern of (a) as-grown and (b) hydrogenated at 30 psi ZnTe/Co bilayer thin films.

### 3.2 I-V Characteristics

Current-voltage characteristics of as-grown and hydrogenated ZnTe/Co BLs thin films are shown in Fig. 2. The hydrogenation pressure dependence on the resistivity ( $\rho$ ) and conductivity ( $\sigma$ ) for ZnTe/Co BLs thin films is shown inset of Fig. 2. It can clearly be seen as the hydrogenation pressure increases from 0 psi to 30 psi, resistivity ( $\rho$ ) increases from  $3.28 \times 10^3$  to  $4.13 \times 10^3 \Omega\text{-cm}$  and therefore conductivity ( $\sigma$ ) decreases from  $3.04 \times 10^{-4}$  to  $2.42 \times 10^{-4} \Omega^{-1}\text{cm}^{-1}$  as shown in Table 1. It may be attributed that hydrogen has controlled the flow of charges by taking electron from Co as anionic model and hydrogen has passivated defect at the interface. Similar results were carried out by Nehra et al. in the case of CdTe/Mn [24], ZnSe/Co [26] BLs and ZnTe/Mn [27], ZnSe/Mn [28] MLs thin films. As-grown and annealed (at 333 K) ZnTe/Co BLs thin films show partially ohmic nature as shown in Fig. 3. Current –Voltage characteristics indicates the mixing of BLs thin films due to annealing because resistivity of annealed ZnTe/Co BLs thin films was found to be decreased from  $3.28 \times 10^3 \Omega\text{-cm}$  to  $3.22 \times 10^3 \Omega\text{-cm}$  therefore conductivity was found to be increased from  $3.04 \times 10^{-4} \Omega^{-1}\text{cm}^{-1}$  to  $3.10 \times 10^{-4} \Omega^{-1}\text{cm}^{-1}$  as shown in Table 1.

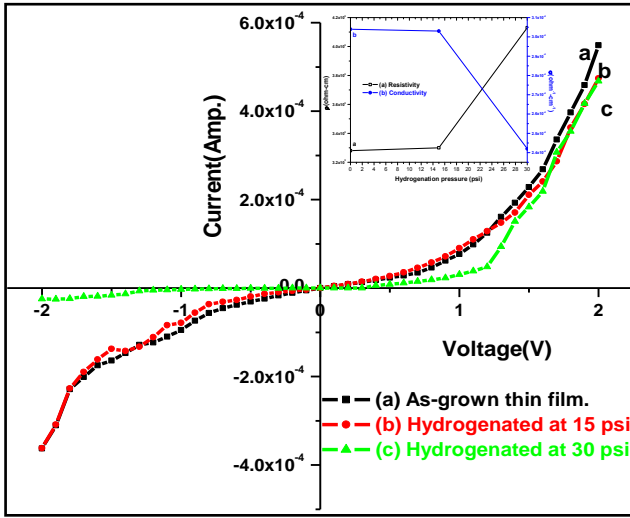


Fig. 2 I-V characteristics of as-grown and hydrogenated ZnTe/Co thin films at different pressure. Inset fig. shows hydrogenation pressure versus electrical resistivity and conductivity plot for ZnTe/Co BLs thin films.

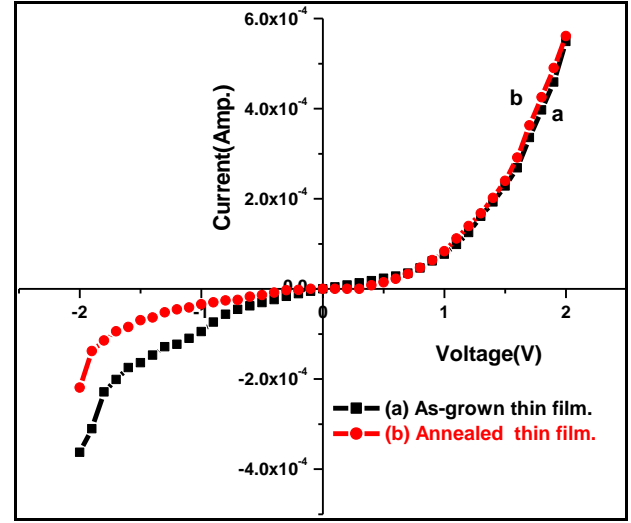


Fig. 3 I-V characteristics of (a) as-grown and (b) annealed at 333K ZnTe/Co BLs thin films.

Table 1. Variation in resistivity and conductivity values for as-grown, annealed and hydrogenated ZnTe/Co BLs thin films.

S. No.	Name of Samples	Resistivity ( $\Omega\text{-cm}$ )	Conductivity ( $\Omega^{-1}\text{cm}^{-1}$ )
1.	As-grown BLs thin film	$3.28 \times 10^3$	$3.04 \times 10^{-4}$
2.	Annealed BLs thin film	$3.22 \times 10^3$	$3.10 \times 10^{-4}$
3.	Hydrogenated at 15 psi	$3.30 \times 10^3$	$3.03 \times 10^{-4}$
4.	Hydrogenated at 30 psi	$4.13 \times 10^3$	$2.42 \times 10^{-4}$

### 3.3 UV-Vis Spectroscopic measurements

Optical absorption spectra of as-grown, annealed and hydrogenated ZnTe/Co BLs thin films are shown in Fig. 4 (a). Hydrogenated BLs thin films show lower absorption comparative to as-grown BLs thin film and absorption increases with increasing hydrogenation pressure. Similar results are observed in the case of CdTe/Mn BLs thin films [25]. Therefore, it may be attributed that hydrogen has passivated defects at the surface or interface of BLs thin films resulting increase in absorption through hydrogenated BLs thin films. It may be attributed that absorption of annealed BLs thin films is lower than as-grown BLs thin films, indicating the mixing of BLs thin films due to the annealing. Due to annealing there is an increase in crystallinity or grain growth resulting reduction in absorption. The nature of the transition can be investigated on the basis of the dependence of the absorption coefficient with the incident photon energy  $h\nu$ . For direct and indirect allowed transitions, the theory of fundamental absorption leads to the following photon energy dependence near the absorption edge:

$$\alpha h\nu = A(h\nu - E_g)^n$$

where  $h\nu$  and  $E_g$  are the photon and band gap energy, respectively. In this relation, the values of  $n$  are 1/2 and 2 for direct allowed and indirect allowed transitions respectively. We have used direct band gap condition for the present study. The plot of  $(\alpha h\nu)^2$  versus  $h\nu$  of as-grown, annealed and hydrogenated ZnTe/Co BLs thin films is shown in Fig. 4(b). Optical band gap of annealed BLs thin film was found to reduce from 3.33 to 3.25 eV due to mixing of semiconductor and metal at the interface and this band gap increased from 3.33 to 3.38 eV in hydrogenated ZnTe/Co BLs thin films with increasing pressure of hydrogenation as shown in the inset of fig.4 (b). It is clearly seen that, with the introduction of hydrogen the band gap of the films is broadened dramatically from 3.34 to 3.38 eV with the increasing hydrogenation pressure 15 to 45 psi. The optical band gaps of as-grown and hydrogenated ZnTe/Co thin films were larger than that of the ZnTe thin films, which is due to band-filling effect known as Burstein-Moss shift [29]. Similar results have also been observed by Tark et al [30] and Hao et al. [31] in the case of effect of hydrogen in

electrical and optical properties of Al-doped ZnO thin films.

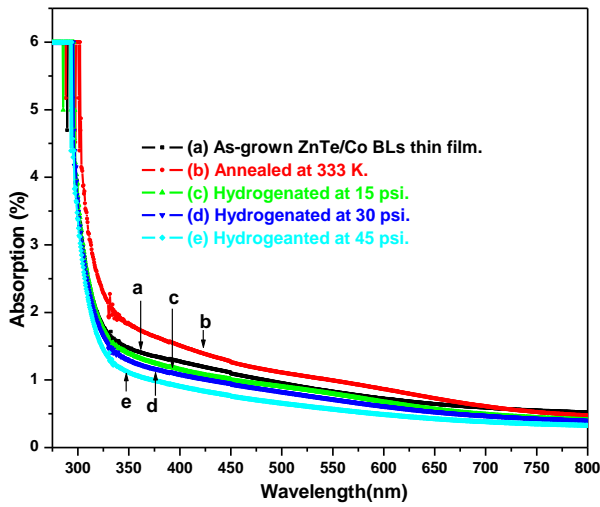


Fig. 4 (a) Wavelength versus absorption plots for ZnTe/Co BLs thin films.

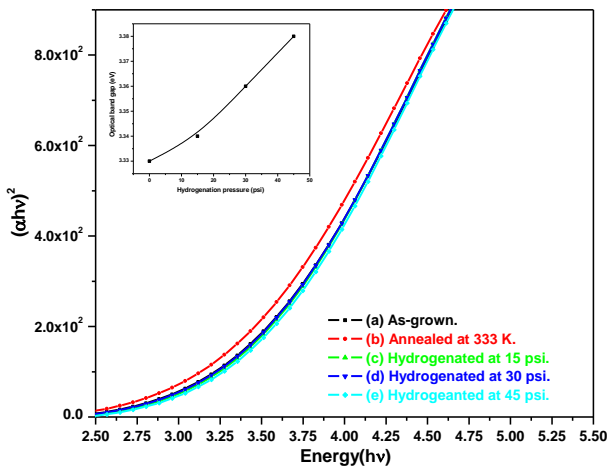


Fig. 4 (b) Optical band gap of as-grown, annealed and hydrogenated ZnTe/Co BLs thin films at different pressure.

### 3.4 Magnetic measurements

The magnetic field dependence of magnetic moment is shown in Fig. 5 and Fig. 6 with the help of temperature vs magnetic moment plots. Magnetic moment decreases with increasing temperature up to 100K after this it becomes constant up to room temperature. ZnTe/Co BLs thin films show paramagnetic nature up to 100 K and after this it becomes saturate. These ZnTe/Co BLs thin films behaves as DMS; that is it does not show any sign of blocking phenomena at very low temperature, and its magnetization does not go to zero and remains constant in the temperature range of 100 to 300 K as suggested by Pakhomov et al [8]. After hydrogenation magnetic moment of these films was found to be reduced with

temperature as well as applied magnetic field. Similar results have also been observed by Liu et al [19]. They found that the saturation magnetization decreases after hydrogenation while the structural properties of the films do not change. Hydrogen passivation is a good method for investigating the origin of ferromagnetism in DMSs. It may be suggested that incorporation of hydrogen electrically passivated the Co acceptors and removes the hole essential to the roaming ferromagnetism. Thus hydrogenation allows us to control the ferromagnetic properties as suggested by Goennenwein et al. [22].

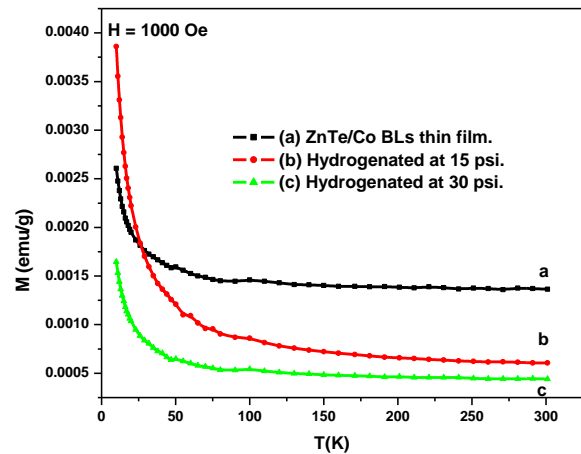


Fig.5 The temperature dependence on magnetization (in ZFC mode) under an applied field of 1000 Oe for as-grown and hydrogenated ZnTe/Co BLs thin films.

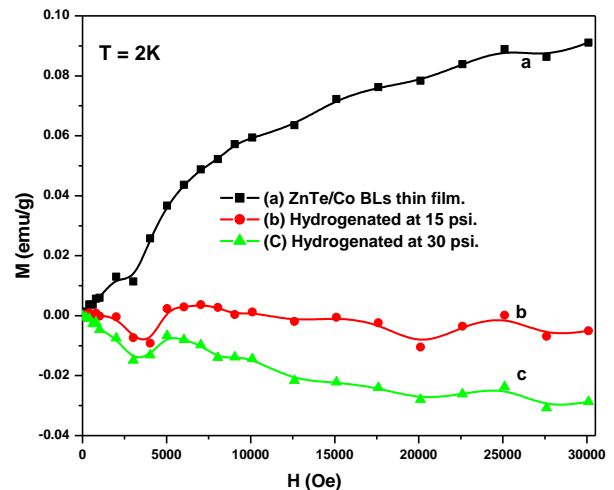


Fig. 6 M- H plots of (a) as-grown, (b) hydrogenated at 15 psi and (c) hydrogenated at 30 psi ZnTe/Co BLs thin films obtained at  $T = 2$  K.

### 3.5 Raman spectroscopy measurements

Raman spectroscopy has been used for confirmation of hydrogen effect on ZnTe/Co BLs thin films. Hydrogen molecules at normal pressure are infrared (IR) inactive due to their lack of dipole moment, but they can be studied by

Raman scattering. Molecular hydrogen was directly observed by Raman spectroscopy. Raman spectra of as-grown and hydrogenated ZnTe/Co thin films are shown in Fig. 7. Comparing the Raman spectra of as-grown and hydrogenated samples it may be concluded that due to the hydrogenation peak intensity and numbers of peaks increases clearly showing the evidence of hydrogenation process. Similar results were observed by Kim [32] and Leitch et al. [33]. Some new peaks were observed at 1019, 1960, 2180, 2680 and 3610  $\text{cm}^{-1}$ . Due to the hydrogenation Raman peak intensity was found to be increased. Similar results were carried out by Nehra et al. in the case of CdTe/Mn [24], ZnSe/Co [26] BLs and ZnTe/Mn [27], ZnSe/Mn [28] MLs thin films. This result indicates that the ZnTe/Co interface was improved due to hydrogenation. This improvement in heterointerface is due to the hydrogenation eliminated defects formed at interface.

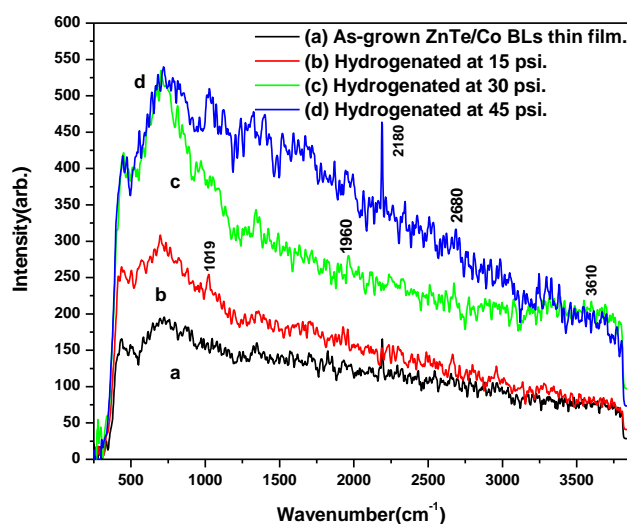


Fig. 7. Room temperature Raman spectra of as-grown and hydrogenated ZnTe/Co BLs thin films.

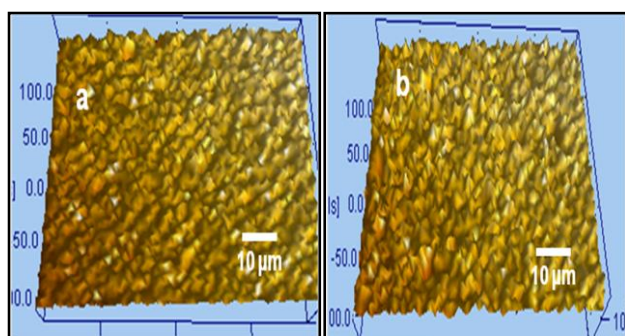


Fig. 8. Surface topography of (a) as grown and (b) vacuum annealed at 333 K ZnTe/Co BLs thin films.

### 3.6 Surface topography

Surface topography of as-grown and annealed ZnTe/Co thin films is shown in Fig. 8 indicating the uniform deposition and mixing of BLs respectively. Due to annealing the crystallinity has found to be increased.

## 4. Conclusions

Thermal evaporation technique has been used to grow ZnTe/Co BLs thin films. Formation of these thin films has been confirmed by XRD and M-H as well as M-T curves. Due to hydrogen passivation effect conductivity and optical band gap have been found to be decreased and increased respectively. Presence of hydrogen in bilayer thin films has also been confirmed by Raman spectroscopy.

## Acknowledgements

The authors are thankful to Department of Physics, Center for Non-Conventional Energy Resources (CNER), University of Rajasthan, Jaipur and Inter University Accelerator Center (IUAC), New Delhi for providing experimental facilities. The authors are also grateful to Tata Institute of Fundamental Research (TIFR), Bombay for SQUID measurements. The authors are highly thankful to University Grant Commission (UGC), New Delhi for providing financial assistance to do this research work.

## References

- [1] P. Sharma, A. Gupta, F. J. Owens, A. Inoue, K. V. Rao, *J. Mag. Magnetic Mater.* **282**, 115 (2004).
- [2] A. F. Orlov, L. A. Balagurov, A. S. Konstantinov, N. S. Perov, D. G. Yarkin, *J. Mag. Magnetic Mater.* **320**, 895 (2008).
- [3] P. YingZi, T. Liew, Y. ZhiZhen, Z. YinZhu, *Chin. Sci. Bull.* **52**, 2742 (2007).
- [4] E. Liu, P. Xiao, J. S. Chen, B. C. Lim, L. Li, *Appl. Phys.* **8**, 408 (2008).
- [5] S. K. Kamila, S. Basu, *Bull. Mater. Sci.* **25**, 541 (2002).
- [6] K. Ando, H. Saito, V. Zayets, M. C. Debnath, *J. Phys. Condens. Matter* **16**, 5541 (2004).
- [7] A. K. Petford-Long, A. N. Chiamonti, *Rev. Mater. Res.* **38**, 559 (2008).
- [8] A. B. Pakhomov, B. K. Bobert, K. M. Krishnan, *Appl. Phys. Lett.* **83**, 4357 (2003).
- [9] D. Ferrand, J. Cibert, A. Wasielea, C. Bourgognon, S. Tatarenko, G. Fishman, *Phys. Rev. B* **63**, 085201 (2001).
- [10] K. V. Brahmam, *Electron. J. Math. Phys. Sci.* **1**, 114 (2002).
- [11] H. J. Lee, C. H. Park, S. Y. Jeong, K. J. Yee, C. R. Cho, M. H. Jung, D. J. Chadi, *Appl. Phys. Lett.* **88**, 062504 (2006).
- [12] K. H. Baik, R. M. Frazier, G. T. Thaler, C. R. Abernathy, S. J. Pearton, J. Kelly, R. Rairigh, A. F.

- Hebard, W. Tang, M. Stavola, J. M. Zavada, *Phys. Lett.* **83**, 5458 (2003).
- [13] C. H. Park, D. J. Chadi, *Rev Lett.* **94**, 127204 (2005).
- [14] M. D. McCluskey, S. J. Jokela, K. K. Zhuravlev, P. J. Simpson, K. G. Lynn, *Appl. Phys. Lett.* **81**, 3807 (2002).
- [15] J. Vetterhöffer, J. Wagner, J. Weber, *Phys. Rev. Lett.* **77**, 5409 (1996).
- [16] L. Thevenard, A. Miard, L. Vila, G. Faini, A. Lemaître, *Appl. Phys. Lett.* **91**, 142511 (2007).
- [17] L. X. Chong, L. Z. Hai, L. Y. Bin, W. J. Feng, L. Z. Lin, L. L. Ya, Y. F. Ming, D. Y. Wei, *Chin Phys B* **18**, 0778 (2009).
- [18] R Farshchi, O. D. Dubon, D. J. Hwang, N. Misra, C. P. Grigoropoulos, *Appl. Phys. Lett.* **92**, 012517 (2008).
- [19] X. C. Liu, Y. B. Lin, J. F. Wang, Z. H. Lu, Z. L. Lu, J. P. Xu, L. Y. Lv, F. M. Zhang, Y. W. Du, *J Appl. Phys.* **102**, 033902 (2007).
- [20] L. Thevenard, L. Largeau, O. Mauguin, A. Lemaître, B. Theys, *Appl. Phys. Lett.* **87**, 182506 (2005).
- [21] S. Y. Park, S. W. Shin, P. J. Kim, J. H. Kang, T. H. Kim, Y. P. Lee, *J Mag. Magnetic Matter.* **310**, e708 (2007).
- [22] S. T. B. Goennenwein, T. A. Wassner, H. Huebl, M. S. Brandt, J. B. Philipp, M. Opel, R. Gross, A. Koeder, S. Wladimir, A. Waag, *Phys. Rev. Lett.* **92**, 227202 (2004).
- [23] K. H. Baik, R. M. Frazier, G. T. Thaler, C. R. Abernathy, S. J. Pearton, J. Kelly, R. Rairigh, A. F. Hebard, W. Tang, M. Stavola, J. M. Zavada, *Appl. Phys. Lett.* **83**, 5458 (2003).
- [24] S. P. Nehra, M. K. Jangid, S. Srivastava, A. Kumar, B. Tripathi, M. Singh, Y. K. Vijay, *Int. J Hyd. Eng.* **34**, 7306 (2009).
- [25] S. P. Nehra, M. Singh, *J Alloys and Comp.* **488**, 356 (2009).
- [26] S. P. Nehra, M. Singh, *Sol. State Commun.* **150**, 1587 (2010).
- [27] S. P. Nehra, M. Singh, *J. Optoelectron. Adv Mater. – Rapid Comm.* **12**, 1125 (2010).
- [28] S. P. Nehra, M Singh, *Vacuum* **85**, 719 (2011).
- [29] E. Burstein, *Phys Rev* **93**, 632 (1954).
- [30] S. J. Tark, Y. W. Ok, M. G. Kang, H. J. Lim, W. M. Kim, D. Kim, *J Electroceram.* **23**, 548 (2009).
- [31] X. T. Hao, F. R. Zhu, K. S. Ong, L. W. Tan, *Semicond. Sci Techno.* **21**, 48 (2006).
- [32] M. D. Kim, H. S. Park, *J. Appl. Phys.* **84**, 3125 (1998).
- [33] A. W. R. Leitch, V. Alex, J. Weber, *Phys. Rev. Lett.* **81**, 421 (1998).

---

\*Corresponding author: nehrasp@gmail.com